SECURITY CLASSIFICATION OF THIS PAGE

REPORT DOCUMENTATION PAGE

1a. REPORT SECURITY CLASSIFICATION Unclassified	1b. RESTRICTIVE MARKINGS
2a. SECURITY CLASSIFICATION AUTHORITY	3. DISTRIBUTION/AVAILABILITY OF REPORT Approved for public release; distribution unlimited
2b. DECLASSIFICATION/DOWNGRADING SCHEDULE	
4. PERFORMING ORGANIZATION REPORT NUMBER(S) Technical Report #7	5. MONITORING ORGANIZATION REPORT NUMBER(S)
6a. NAME OF PERFORMING ORGANIZATION Materials Engineering Dept. RPI	6b. OFFICE SYMBOL (If applicable)
6c. ADDRESS (City, State and ZIP Code) Troy, NY 12180-3590	7a. NAME OF MONITORING ORGANIZATION Office of Naval Research
	7b. ADDRESS (City, State and ZIP Code) Chemistry Program 800 N. Quincy Street Arlington, VA 22217
8a. NAME OF FUNDING/SPONSORING ORGANIZATION Office of Naval Research	8b. OFFICE SYMBOL (If applicable)
8c. ADDRESS (City, State and ZIP Code) Chemistry Program 800 N. Quincy St. Arlington, VA. 22217	9. PROCUREMENT INSTRUMENT IDENTIFICATION NUMBER Contract # N00014-86-K-0259
	10. SOURCE OF FUNDING NOS.

PROGRAM ELEMENT NO.	PROJECT NO.	TASK NO.	WORK UNIT NO.
NR	056	533	

11. TITLE (Include Security Classification)
THE TITRATION OF OXYGEN ON A POLYCRYSTALLINE IRON SURFACE BY PERMEATING HYDROGEN

12. PERSONAL AUTHOR(S)
Mehran Arbab and John B. Hudson

13a. TYPE OF REPORT	13b. TIME COVERED	14. DATE OF REPORT (Yr., Mo., Day)	15. PAGE COUNT
Interim Technical	FROM 3/1/86 TO 2/28/88	1988-2-28	45

16. SUPPLEMENTARY NOTATION
Submitted to Surface Science

17. COSATI CODES			18. SUBJECT TERMS (Continue on reverse if necessary and identify by block number)
FIELD	GROUP	SUB. GR.	Surfaces, chemistry, kinetics, adsorption, hydrogen, oxygen, metals
Surface	Reactions		

19. ABSTRACT (Continue on reverse if necessary and identify by block number)

The interaction between oxygen and hydrogen on a clean polycrystalline iron surface was studied by Auger electron spectroscopy and mass spectrometry. To avoid having the reaction kinetics limited by the slow adsorption of hydrogen on the oxidized surface, hydrogen was supplied by permeation through the thin iron specimen. For oxygen coverages of more than one monolayer, this procedure resulted in the rapid titration of oxygen by the formation and desorption of water. In the temperature range of 475-625 K, the reaction path consists of the initial formation of OH from coadsorbed oxygen and hydrogen, followed by the disproportionation of two hydroxyl species to form H_2O. An overall activation energy of 7-8 Kcal/mole was measured for the above reaction sequence. Oxygen in coverages of less than one monolayer could not be removed by hydrogenation, in agreement with a previous study on an Fe(100) single crystal substrate. The present study shows that this apparent stability of the chemisorbed oxygen is not due to the kinetics of hydrogen adsorption.

20. DISTRIBUTION/AVAILABILITY OF ABSTRACT	21. ABSTRACT SECURITY CLASSIFICATION
UNCLASSIFIED/UNLIMITED ☒ SAME AS RPT. ☒ DTIC USERS ☐	Unclassified

22a. NAME OF RESPONSIBLE INDIVIDUAL	22b. TELEPHONE NUMBER (Include Area Code)	22c. OFFICE SYMBOL
Dr. David L. Nelson	(202) 696-4410	

OFFICE OF NAVAL RESEARCH

Contract N00014-86-K-0259

Task No. NR-056-533

TECHNICAL REPORT NO. 7

THE TITRATION OF OXYGEN ON A POLYCRYSTALLINE IRON SURFACE BY PERMEATING HYDROGEN

BY

Mehran Arbab* and John B. Hudson
Materials Engineering Department
Rensselaer Polytechnic Institute
Troy, NY 12180-3590

*Present Address:
Materials Engineering Department
Case Western Reserve University
Cleveland, OH 44106

February 28, 1988

Abstract

The interaction between oxygen and hydrogen on a clean polycrystalline iron surface was studied by Auger electron spectroscopy and mass spectrometry. To avoid having the reaction kinetics limited by the slow adsorption of hydrogen on the oxidized surface, hydrogen was supplied by permeation through the thin iron specimen. For oxygen coverages of more than one monolayer, this procedure resulted in the rapid titration of oxygen by the formation and desorption of water. In the temperature range of 475-625 K, the reaction path consists of the initial formation of OH from coadsorbed oxygen and hydrogen, followed by the disproportionation of two hydroxyl species to form H_2O. An overall activation energy of 7-8 Kcal/mole was measured for the above reaction sequence. Oxygen in coverages of less than one monolayer could not be removed by hydrogenation, in agreement with a previous study on an Fe(100) single crystal substrate. The present study shows that this apparent stability of the chemisorbed oxygen is not due to the kinetics of hydrogen adsorption.

1- Introduction :

The study of the interaction between hydrogen and oxygen on transition metal surfaces is important to the understanding of heterogeneous catalysis. The consideration of this reaction on iron is additionally motivated by its relevance to the aqueous corrosion of ferrous alloys.

There have been a number of studies of the interaction of water with iron surfaces of different orientations [1-4], which we will consider in a later section. There are, on the other hand, only few examples of similar studies of the interaction between oxygen and hydrogen on iron. Vink and coworkers have considered this problem on the (100) [5a] and (110) [5b] surfaces of iron, using ellipsometry and Auger electron spectroscopy (AES). In their work, oxidized surfaces were prepared by exposure to oxygen at room temperature until a saturated oxide overlayer was obtained. This step was followed by a high temperature anneal prior to the reduction of the oxide by hydrogen. On both surfaces the reaction reached completion only after large hydrogen exposures, achieved by hydrogen partial pressures of $1x10^{-3}$ torr or higher. The two substrates differed in one important aspect: While it was possible to remove all of the adsorbed oxygen from the (110) surface, one monolayer of adsorbed oxygen always remained on the (100) surface, independent of exposure or the substrate temperature.

The exposures necessary to completely remove the titratable oxygen from a particular surface exceeded the initial surface oxygen concentration by many orders of magnitude. This may have been due to

the small sticking coefficient for hydrogen adsorption on an oxidized iron surface [23].

If the above assumption is valid, a means of increasing the supply of hydrogen adsorption at the surface should facilitate the titration process. For example, Mesters et al. [6] determined that the titration of oxygen *from* a Cu(111) surface by gas phase molecular hydrogen has an apparent activation energy of approximately 15 Kcal/mole. However, this value dropped to about 1 Kcal/mole when an ion gauge was turned on. They interpreted their data using a kinetic model which required site blocking for the dissociative adsorption of hydrogen by the pre-adsorbed oxygen. This requirement was not necessary for the interpretation of data obtained with the gauge on. Therefore, they concluded that in the presence of pre-adsorbed oxygen, hydrogen adsorption was the rate limiting step and that the excitation of hydrogen molecules at the ion gauge removed the barrier to dissociative adsorption.

In the case of iron, as well as a number of other metals (e.g. Pd and Ni), hydrogen is known to be a very fast diffuser [7]. This suggests that permeation across a thin metal membraneone is a possible route for sustaining a large atomic hydrogen concentration on the reaction surface. This idea was adopted in the present work. The results, which confirmed the above hypothesis, are described below. This method has two additional advantages over high pressure studies: first, surface contamination by residual gases, which is possible at high pressures, will be small at the low pressures encountered here (less than $1x10^{-7}$ torr); also, the in situ use of many surface techniques that require high vacuum will be possible.

The present study differs from those of Vink et al. [5] in the choice of the initial oxygen coverage. We have considered only those coverages that are small enough to allow for the determination of the oxygen concentration by AES, as will be detailed below. The initial concentration chosen by the above authors on the other hand, was the maximum amount of oxygen that could be adsorbed in a UHV environment at room temperature. The two studies should, therefore, be viewed as complementary to each other.

2. EXPERIMENTAL:

A detailed description of the apparatus used in this study has been presented elsewhere [8]. Briefly, the all stainless steel ultrahigh vacuum system was comprised of two chambers, which were interconnected through a 1.45 mm diameter orifice. The ion-pumped main chamber was equipped with a cylindrical mirror electron energy analyzer with a co-axial electron gun for Auger electron spectroscopy (AES), an ion gun for sputter cleaning of the sample surface, and the sample manipulator. A base pressure of 5×10^{-10} torr could be attained after bake out. The detector chamber housed a quadrupole mass spectrometer (QMS) and was independently evacuated by a cryopump to a base pressure of better than 2×10^{-10} torr (ionization gauge limit).

The hydrogen permeation assembly was constructed by TIG welding the high purity, 1 mm thick polycrystalline iron sample (MARZ Grade, Materials Research Corporation) to a low carbon steel cell. The sample was heated by electron bombardment from the backside of the cell. Its temperature was monitored by a W-5%Re, W-26%Re

thermocouple spot welded near the front of the cell. The surface of the sample was cleaned by repeated cycles of argon ion sputtering and annealing in vacuum until the coverage of all surface contaminants were reduced to at most a few atomic percent, as determined by AES.

Optical microscopy of the sample after the completion of experiments showed it to be comprised of coarse grains, about 20% of which had average diameters of 1 mm or larger. An average ASTM grain size of 5 was estimated for the specimen. Laue x-ray diffraction patterns taken on various spots on the sample indicated no preferred orientation. In one instance, diffraction from one or more of the larger grains resulted in a well defined pattern characteristic of a high index plane (a (429) orientation). The (429) plane can be envisaged as (001) terraces separated by (210) steps, where for monatomic step heights the terraces will be alternatively 4 and 5 atomic rows wide, the rows defining the <120> direction. The (210) orientation may in turn be thought of as regularly spaced (100) steps and (010) kinks.

Gases were admitted to the main chamber via leak valves. Partial pressures were measured by an ionization gauge calibrated according to the manufacturer's specifications. In the case of oxygen, and particularly at pressures exceeding 10^{-8} torr, this method was observed to be unreliable and often to result in the overestimation of the partial pressure. Therefore, the QMS was calibrated against the ionization gauge at pressures below 10^{-8} torr, where the correspondence between the outputs of the two instruments was linear, and was subsequently employed for P_{O2} measurements. While utilizing the mass spectrometer for this purpose

results in a precise determination of the relative changes in the partial pressure of oxygen, the accuracy in absolute partial pressure measurements will continue to depend on the sensitivity of the ionization gauge, and the extent of backstreaming of other gases from the ion pump, at low presssures.

The mass spectrometer was also used for measuring the rate of water evolution from the surface of the iron sample due to the interaction between oxygen and hydrogen. The differential pumping of the QMS was essential in separating the water signal, due to the above reaction on the surface of interest, from a time dependent background due to reactions occuring on other surfaces. In spite of this arrangement, a number of steady state experiments required an independent determination of the spurious contributions to the QMS water signal. The procedure adopted has been described previously for similar steady state measurements of hydrogen permeation [8].

The coverage of oxygen on the iron surface was followed by measuring the ratio of the height of the instantaneous oxygen KLL peak (503eV), I_O, to that of the iron LMM peak (703eV), I_{Fe}, as measured on a clean surface prior to each run. This ratio, which we shall refer to as I^* hereafter, was not independently calibrated, but was assumed [16] to be proportional to the oxygen coverage on the sample surface, θ:

$$I^* = I_O / I_{Fe} = \beta\theta, \qquad (1)$$

where β is an undetermined constant of calibration. All Auger spectra were obtained using a 6 eV peak to peak modulation of the CMA pass

energy, except for the fine structure analysis of the 47 eV Auger peak of iron, where a 1 eV modulation was used.

3. Results:

The experiments that to be described below followed independent studies of hydrogen permeation through the iron sample [8] and the adsorption of oxygen on its surface [9], both using the same sample as the present work. We will begin this section by summarizing those aspects of the above studies that are pertinent to this work.

3.1.1. Hydrogen Permeation:

For temperatures above 475 K, the steady state permeation of hydrogen through the iron sample was found to conform to the usual Arrhenius behavior, as expected from a diffusion controlled process. The activation energy for permeation in this high temperature range was 8.5±0.4 Kcal/mol, in good agreement with a number of earlier studies of this system [7].

At lower temperatures, the desorption of hydrogen from the surface of the sample controlled the permeation rate, leading to overall activation energies larger than those expected from the extrapolation of the high temperature data [8].

To simplify data analysis in the present study, we chose the point of the above deviation from Arrhenius behavior as the lower limit for oxygen titration experiments.

3.1.2. Oxygen Adsorption:

Oxygen uptake was observed to proceed in three distinct adsorption regions [9]. For Auger spectra taken in the derivative mode, The iron MVV peak appears at 47 eV. The fine structure of this Auger feature is sensitive to the oxidation state of the substrate; an oxide is characterized by a peak lower in energy than 47 eV [10]. By carefully recording the structure of the iron MVV peak at various oxygen coverages, it was possible to identify the three adsorption regimes as chemisorption of oxygen, in the first region, followed by the oxidation of the substrate in the two subsequent stages. The transition from stage one to stage two occured in the range of $0.17 \leq I^{*} \leq 0.21$.

The normalized oxygen Auger peak height, I^{*}, was translated into oxygen coverage in the following manner [9]: a plot of the intensity of the iron MVV peak at 47 eV, (i.e. that due to electrons originating in the metallic substrate), against I^{*} could be fitted to a simple exponential model of intensity attenuation versus overlayer thickness. The fit resulted in a value of I^{*} equivalent to the inelastic mean free path (IMFP) of the 47 ev electrons through the oxidized overlayer. A comparison of this value with the independently measured value of the IMFP, namely 4.7 A° [11], provided an estimate of oxygen coverage (see ref. 9). In this manner the transition from region I (chemisorption) to region II (oxidation) was determined to occur at an oxygen coverage of 0.8-1.0 monolayers, in agreement with earlier results on Fe(100) substrates [12,13].

The adsorption probability beyond chemisorption, during the

early stage of oxidation, was independent of oxygen coverage on the surface; that is, for a given oxygen partial pressure (P_{O2}) the rate of uptake was independent of time. Moreover, the rate of adsorption in this period was proportional to P_{O2}, but decreased as the substrate temperature was increased. These three observations can be explained in terms of a model that describes the incorporation of oxygen molecules into the subsurface oxide as a three step process: i- the adsorption of the oxygen molecule on the surface (precursor formation), ii- the dissociatior of the molecule into two adsorbed atoms, and iii- the incorporation of the adsorbate into the subsurface region in a direction normal to the surface of the substrate, where the last step is assumed to be non-activated [14]. The population of the precursor species, [P'], is assumed to reach a small steady state value rapidly (the steady state approximation [15]). Under these conditions, [P'] and the rate of oxygen uptake can be expressed by the following two expressions [4]:

$$[P'] = \frac{a'Z}{k'_d + k'_a}, \tag{2}$$

and

$$\frac{d[O_{ox}]}{dt} = SZ = \frac{2a'Z}{1+(k'_d/k'_a)}. \tag{3}$$

where Z, the impingement rate, is proportional to the partial pressure of oxygen, and a', k'_a, and k'_d are the trapping probability, and the dissociation and desorption rate constants for the molecular precursor, respectively. (the primes distinguish these parameters from those describing the chemisorption period. They are used here for consistency with the original paper [9].)

The analysis of the kinetics of oxygen uptake or titration beyond the linear adsorption period is complicated by the fact that the limited IMFP of the Auger electrons will contribute to any apparent decrease in the corresponding rates. The oxygen titration data presented here are, therefore, those with initial oxygen coverages within the first two stages of adsorption, i.e. corresponding to an I^* value of about 0.55 or less.

3.2. The Hydrogen-Oxygen Reaction:

The exposure of an oxygen covered sample to several thousand Langmuirs of gas phase hydrogen (in excess of $9x10^3$L) did not result in any detectable loss of oxygen from the surface beyond that caused by dissolution [9]. The extent of initial oxygen coverage had no effect on this behavior. Moreover, the slow dissolution of oxygen into the substrate obscures the competing process of oxygen removal by titration, if long term exposures of the sample to low hydrogen pressures are used (cf. fig. 3).

In contrast to the above experiments, atomic hydrogen [8] arriving at the surface by permeation from the back-side of the sample reacted rapidly with the pre-adsorbed oxygen and resulted in the formation and desorption of water molecules. The variations in I^* as a function of time for various initial oxygen coverages, at 550 K, are shown in Figure 1. These results indicate that the reaction proceeds until a fixed value of I^*_f, equal to about 0.18, is reached. This value of I^*, which is independent of the initial coverage, corresponds to approximately 1 monolayer of oxygen,

according to the calibration procedure described in sec. 3.1.2 and in reference 9. In addition, when a sample with an initial oxygen coverage below I^*_f is exposed to atomic hydrogen by permeation, no reaction is observed.

Figure 2 represents the effect of temperature on this reaction in the range of 475 to 625 K, for a given initial value of oxygen coverage. It is again observed that, despite an increase in the reaction rate, the removal of oxygen does not proceed beyond the value of I^*_f observed in the previous set of experiments. Irrespective of the substrate temperature, the reaction results in the removal of all the adsorbed oxygen in excess of I^*_f. The initial oxygen coverage for this set of experiments was I^*_o=0.425. (This value of I^* corresponds to an oxide thickness of approximately 2.4-2.9 A°, beneath the chemisorbed oxygen layer [9].) The effect of temperature on the magnitude of I^* as a function of time, and in the absence of hydrogen, is shown for two different temperatures in Figure 3. The rate of decrease in I^* due to incorporation of oxygen into the metal is small relative to its change due to the reaction of oxygen with hydrogen.

An inspection of the iron MVV Auger peak after the completion of the reaction (see sec. 3.1.2) showed the remaining oxygen to be chemisorbed rather than an oxide anion. Similarly, the value of I^*_f was consistently found to be within the chemisorption-oxidation transition range of oxygen adsorption, as discussed above ($0.17 \leq I^* \leq 0.21$). Therefore, we conclude that, in the temperature range considered in this work, the removal of chemisorbed oxygen from this particular iron surface by hydrogenation is immeasurably slow.

The rate of water evolution from the sample during the titration process was measured by the QMS. Typical examples are shown in Figure 4. The initial oxygen coverage for these experiments was the same as that shown in Figure 2. In each experiment, the adsorption period was monitored by AES. Following the accumulation of a pre-determined amount of oxygen, the sample was rotated by 180° to face the orifice of the mass spectrometer. Its position was then adjusted for a maximum QMS intensity, as determined in preliminary experiments. The time interval allotted for this procedure was one minute. Thus, for consistency in experiments, a corresponding one minute delay between the adsorption and titration periods was also included in the above AES studies.

Two groups of steady state experiments were performed at a substrate temperature of 550 K (i.e. the mid-range of the temperatures that were considered). In both cases, the rate of hydrogen permeation was allowed to reach its steady state value before the chamber was backfilled with a constant partial pressure of oxygen. Figure 5 shows that the ensuing rate of water production at steady state increases with increasing P_{O2}. As indicated on the figure, a slope of 0.8±0.1 was obtained by least squares analysis of the rate versus partial pressure data. This value is, however, only approximate since during these experiments the QMS was used for measuring the rate of water formation, and therefore P_{O2} was determined by the ionization gauge in the main chamber. This practice introduces some error in the measurement of the actual changes in the value of P_{O2}, as explained in section 2.

In the second set of experiments, the mass spectrometer was employed for P_{O2} measurements, while the concentration of oxygen on the surface (I^*), as a function of oxygen partial pressure, was measured by the Auger spectrometer. It was found that upon the exposure of the sample to oxygen, I^* increased with time to attain a steady state value always equal to or greater than I^*_f. The magnitude of coverage in excess of I^*_f at different partial pressures of oxygen is shown in Figure 6. Since only the relative changes in P_{O2} are important to these experiments, the uncalibrated QMS oxygen signal is shown on the abscissa. The data indicate that the above conditions yield a steady state magnitude of $(I^*-I^*_f)$ which increases linearly with the square root of oxygen partial pressure.

4- Kinetic Model and Analysis:

Any description of a heterogeneous reaction between two or more gas species should address the question of whether or not every reactant has to adsorb on the surface prior to other interactions. A number of previous investigations of the reaction between hydrogen and oxygen on various metal surfaces have generally shown that this reaction requires both species to be adsorbed on the metal surface before they can react with each other. In this study, however, as the hydrogen species permeates through the bulk and arrives at the surface as atoms, and since the oxygen species is already adsorbed on the surface, the above question does not arise.

Thus, the following three schemes were considered in order to

explain the results of hydrogen-oxygen interactions:

$$(O)_{ad}+2(H)_{ad} \longrightarrow H_2O \qquad (I)$$

$$(O)_{ad}+(H)_{ad} \longrightarrow (OH)_{ad} \qquad (IIa)$$

$$(OH)_{ad}+(H)_{ad} \longrightarrow H_2O \qquad (IIb)$$

$$(O)_{ad}+(H)_{ad} \underset{k_{-1}}{\overset{k_1}{\rightleftharpoons}} (OH)_{ad} \qquad (IIIa)$$

$$(OH)_{ad}+(OH)_{ad} \xrightarrow{k_2} H_2O+(O)_{ad} , \qquad (IIIb)$$

where $(O)_{ad}$ refers to the titratable oxygen on the surface (see below).

With equivalent sets of assumptions, only the third reaction scheme provides an adequate description of our results. We will now consider the assumptions leading to the final kinetic expression in some detail.

4.1- The AES Data:

Within the temperature range of this work ($T \geq 475$ K), the desorption of water from the surface occurs rapidly relative to the steps leading to its formation [17]. Similarly, the surface recombination of the permeating hydrogen atoms and the desorption of the H_2 molecules thus formed are assumed to be rapid in comparison with the permeation process above 475 K. We have already shown this assumption to be valid with respect to a clean surface [8]. Therefore, the concentration of the hydrogen adspecies will depend on the hydrogen flux at the reaction interface, J, at time t (it will be shown below that the contribution from step IIIa to hydrogen coverage

will drop out as the result of an assumption concerning [OH_{ad}]). That is:

$$[H_{ad}]^2=J/k_d \qquad (4)$$

where k_d is the rate constant for hydrogen desorption.

In sec. 3.2 it was shown that the titration process is incomplete, and, as evidenced by the fine structure of the MVV Auger peak of the iron substrate, the remaining oxygen is chemisorbed. This observation coincides with the finding of Vink et al. [5] about the same interaction on an Fe(100) surface.

It is not immediately clear whether the final untitrated species occupies the same surface site throughout the reaction period, or a subsurface oxide anion migrates to the chemisorption site only at the end of the titration process. Further insight may be gained by considering those expeiments where the initial oxygen coverage was equal to or less than one monolayer, i.e. the coverage at the end of the chemisorption period. In these experiments no change in the oxygen coverage during hydrogen permeation was noted, even for extended permeation times at high temperatures. Therefore, the chemisorbed oxygen can not be removed by hydrogen. The formation of another stable surface species, such as a hydroxyl group, can not be overruled at this time.

Also, in a previous discussion regarding the sequential nature of oxygen adsorption on iron [9], we showed that upon exposing a clean substrate to oxygen, the formation of a two dimensional, subsurface, oxide phase begins only after a majority of the

chemisorption sites are populated. Based on a review of a number of previous studies, we assumed that the chemisorbed oxygen remains stable relative to the oxide phase, at least during the initial oxidation period. The incorporation of oxygen into the 2D oxide was proposed to follow the dissociative adsorption of O_2 on surface sites distinct from the chemisorption sites. In agreement with this model, and in view of the above experiments, we concur with Vink et al. [5a] in assuming that the chemisorbed oxygen is never a direct participant in the titration process. Hence, the population of the "titratable" species on the surface is in equilibrium with the oxide oxygen atoms that were adsorbed following the chemisorption period, O_{ad}, with an equilibrium constant of K. According to steps a and b of reaction III, the variation in the concentration of the adsorbed oxygen and hydroxyl species as a function of time can be then written as:

$$d[O_{ad}]/dt=-k_1K[O_{ad}][H_{ad}]+k_{-1}[OH_{ad}]+k_2[OH_{ad}]^2 \quad (5)$$

and

$$d[OH_{ad}]/dt=k_1K[O_{ad}][H_{ad}]-k_{-1}[OH_{ad}]-2k_2[OH_{ad}]^2, \quad (6)$$

(Recall that we have defined $[O_{ad}]$ as the concentration of titratable oxygen atoms).

In our experiments, however, it was not possible to determine the populations of the oxygen and hydroxyl adspecies independently from each other; the Auger parameter, I^* is proportional

to the total concentration of oxygen species on the surface. Hence:

$$I^*-I^*_f = \beta\{[O_{ad}]+[OH_{ad}]\}, \qquad (7)$$

where β is a constant of calibration for AES (sec. 2), and I^*_f corresponds to the final oxygen concentration remaining on the surface: $(I^*-I^*_f)$ is proportional to the titratable oxygen concentration. Therefore:

$$d(I^*-I^*_f)/dt = \beta\{\, d[O_{ad}]/dt+d[OH_{ad}]/dt \,\}. \qquad (8)$$

Thus, according to Equations 5 and 6, we have:

$$d(I^*-I^*_f)/dt = -\beta k_2[OH]^2 \qquad (9)$$

At this point we will assume that the population of the hydroxyl species on the surface rapidly reaches steady state and that its coverage is always much smaller than one monolayer -i.e. $[OH_{ad}]<<N_o$, where N_o is the planar density of adsorption sites on the surface. This assumption implies that the forward step IIIa is slow relative to the disproportionation step, IIIb (see below). Equation 6 may now be rewritten by setting $d[OH_{ad}]/dt$ to zero. With some further rearrangement of the parameters we have:

$$k_1K[O_{ad}][H_{ad}]=2k_2N_o\{(k_{-1}/2k_2N_o)+[OH_{ad}]/N_o)\}[OH_{ad}]. \qquad (10)$$

If $k_{-1}{}^o$, the pre-exponential factor for the first order

dissociation process of the hydroxyl species, and $k_2{}^{o}N_o$ are taken to be approximately equal, then for $H_2 \geq H_{-1}$, we may write:

$$[OH_{ad}]=(k_1K/k_{-1})[O_{ad}][H_{ad}]. \qquad (11)$$

The assumption of the above inequality is in agreement with the theoretical results of Anderson [18a] and Debnath and Anderson [18b]. In a study of water adsorption on Fe(100), Anderson found an activation energy of 0.64 ev for the dissociation of the hydroxyl radical (H_{-1}) adsorbed on a Fe_5 cluster, while the latter authors calculated an activation energy of 1.5 ev or more for the disproportionation reaction (H_2) on a Fe_9O_{13} cluster, or 0.9 ev on a Fe_5O cluster [18a]. In addition, the activation energy for the forward reaction, IIIa, on an Fe_5 cluster was found to be approximately 3 ev, making it slow relative to the reaction step IIIb, or the reverse reaction IIIa. This provides support for our assumption regarding the small steady state concentration of the OH radicals.

A consequence of Equation 11 is that step IIIa is always in equilibrium. Therefore, expression 4, which describes the concentration of the hydrogen adspecies without accounting for contributions from reaction IIIa, is satisfied.

Equation 9 may now be written in terms of the expression for $[OH_{ad}]$ given by Equation 11. With the further approximation of $(I^*-I^*_f) = \beta[O_{ad}]$, in agreement with the assumption concerning $[OH_{ad}]$, we can write:

$$d(I^*-I^*_f)/dt=-\beta^{-1}k_2(k_1K/k_{-1})^2(I^*-I^*_f)^2[H_{ad}]^2. \quad (12)$$

The expression for permeation through a semi-infinite membrane of thickness L is given by Crank [29]. It may be written in the form appropriate to the present problem as:

$$J=(C_1D/L)\{1+2\sum_1^\infty(-1)^n\exp(-Dn^2\pi^2t/L^2)\}, \quad (13)$$

where C_1 is the hydrogen concentration just below the back surface of the sample, in contact with one atmosphere of hydrogen. Its value depends on the solubility of hydrogen in iron. Hydrogen diffusivity in iron is shown by D in the above equation.

Using Equations 4 and 13, Equation 12 may now be solved for I^* as a function of time:

$$I^*=\frac{1}{\frac{1}{I_o^*-I_f^*}+B[t+(2L^2/\pi^2D)\sum_1^\infty\frac{(-1)^n}{n^2}\exp(-n^2\pi^2Dt/L^2)+L^2/6D]}+I_f^* \quad (14a)$$

where I_o^* refers to the initial oxygen coverage on the surface, including the untitratable oxygen coverage. The parameter B in Equation 14a is an exponential function of 1/T which includes a number of previously defined rate constants:

$$B=(k_2k_1^2K^2C_1D)/(Lk_dk_{-1}^2\beta) \quad (14b)$$

The summation terms in Equation 14a decrease linearly with n^{-2} and exponentially with n^2. Therefore, we will approximate the

sum by its first term only. (A numerical examination of the sum reveals this approximation to be very good for times exceeding a few seconds and for $T \geq 475$ K.)

Equation 14a, was fitted to the oxygen removal data obtained by AES with the use of the above approximation and a least squares method (Levenberg-Marquardt algorithm), and is shown as solid lines in Figure 2. An excellent description of the experimental data, at all temperatures involved, was obtained by adjusting the parameters B and I_f^*. The average value of I_f^* obtained as the result of this procedure was 0.18±0.01, in agreement with experiment. Calculated values of ln(B) are plotted in Figure 7 as a function of 1/T. Linear regression analysis of this data yields an activation energy of 16±2.6 Kcal/mol for the process. The activation energy for hydrogen permeation in iron was independently measured as 8.5±0.4 Kcal/mol [8]. Hence, the overall activation energy for steps a and b in reaction path III, above, is about 7±2.7 Kcal/mol. This value is in good agreement with the value of 11.5 Kcal/mol, measured by Villarrubia and Ho [19], for the activation energy for H_2O formation by the reaction of gas-phase hydrogen with oxygen chemisorbed on Ni(110).

4.2- The QMS data:

According to step IIIb, the rate of water formation as a function of time can be written as:

$$d[H_2O]/dt = k_2[OH]^2. \qquad (15)$$

Employing the previous approximations for $[OH_{ad}]$, $[H_{ad}]$, and J, and substituting I_w for $d[H_2O]/dt$, where I_w is the mass spectrometer signal for water desorbed from the reaction surface (counts/sec) and is an undetermined constant of calibration for that signal, we obtain:

$$I_w=B'(I^*-I_f^*)^2\{1+2\sum_{1}^{\infty}(-1)^n\exp(-n^2\pi^2Dt/L^2)\} \qquad (16)$$

In the above expression B' is related to B by the constant $/\beta$.

The sum in Equation 16 was approximated, rather arbitrarily, by its first three terms, as the decrease in the successive terms depends only exponentially on n^2 and, therefore, occurs more slowly than in Equation 14a. Equation 16 was fitted to the data presented in Figure 4 by adjusting B' and using the AES data (Figure 2) taken at the same temperature as the corresponding QMS data, during an independent run. It is clear that such an analysis suffers from the uncorrelated scatter in the two sets of data. In addition, the QMS measurements were recorded every one second, while the AES data could be recorded only at 2.5 second intervals or longer. This, in association with the uncertainty of 1-2 seconds in initiating the titration process, i.e. opening the valve to the hydrogen reservoir to pressurize the permeation cell, introduces additional error into the above analysis. Nonetheless, a plot of the LHS of Equation 16, i.e. the rate of H_2O formation as measured by the mass spectrometer, versus its RHS, which predicts the rate of H_2O formation by hydroxyl disproportionation at a given oxygen coverage, indicates a

good correlation between the the results of these independently-performed groups of experiments (Figure 8). A least squares analysis of this data yields the slope of the solid lines which are also shown in Figure 8. These slopes were assumed to be equivalent to B'.

The plot of ln(B') versus 1/T is shown in Figure 9. Linear regression analysis of this data results in an activation energy of 16.4±3.2 for water formation in association with hydrogen permeation, which agrees well with the independent evaluation of the AES data.

4.3- The Effect Of The Initial Oxygen Concentration:

For experiments performed with an initial oxygen coverage within the linear oxidation period (Figure 1), Equation 14 could be fitted to the data for all values of I_o^*. The value of the fitting parameter B, however, decreased exponentially as the initial oxygen coverage was increased (Figure 10). At 550 K the relationship between the above two parameters may be written as:

$$\ln(B_{550})=2.27-7.44I_o^*. \qquad (17)$$

Keeping in mind that B is an Arrhenius function of temperature, we may write:

$$-H_B=550R(2.27-7.44I_o^*-\ln B_o). \qquad (18)$$

That is, the reaction energy depends on the initial extent of

oxidation. For an initial oxygen coverage of I^*=0.425, H_B may be evaluated from the above equation if B_o is replaced by its value from the plot of ln(B) versus 1/T in Figure 7. The result that H_B=15.9 Kcal/mol is consistent with our two previous determinations of this parameter.

Data shown in Figure 10 include the results of titration experiments by both hydrogen and deuterium permeation. No isotope effect is apparent in these results. On the other hand, Equation 14b indicates that as the activation energies for hydrogen (deuterium) permeation and desorption become respectively smaller and larger the overall reaction energy, H_B, should decrease. If other parameters remain constant, these conditions would favor a larger coverage of hydrogen on the surface (Equation 4), a condition that should result in a faster titration reaction. Previous studies of these two isotopes on iron indicate that deuterium permeates [20] with a larger activation energy and desorbs [21] with a smaller activation energy than hydrogen. These results predict H_B to be larger for deuterium than hydrogen by up to 1.3 Kcal/mole. This value is small enough to fall within the uncertainty range of our measurements. The expected effect of deuterium in reducing the rate of oxygen removal has been recently observed on a Rh(100) surface, at cryogenic temperatures, by Gurney and Ho [22]. In addition to the desorption parameter discussed above, these authors infer an increase in the activation energy for the formation of the OD species over that for OH formation (i.e. an increase in H_1, in Equation 14b).

4.4- Steady State Measurements:

The half order dependence of $(I^*-I^*_f)$ on oxygen partial pressure during the steady state permeation of hydrogen (Figure 6) can be explained in terms of the combination of the hydroxyl disproportionation mechanism, described above, and the non-activated place exchange model of the initial oxidation of iron, which has been discussed in detail elsewhere [9] and reviewed briefly in sec. 3.1.2. As the clean surface is exposed to oxygen during the steady flow of hydrogen to the surface, the chemisorption sites will be preferentially occupied and approach saturation. The molecular oxygen precursors that are adsorbed subsequently will dissociate and either be removed from the surface by the hydrogenation and disproportianation process, or, alternatively, will be incorporated into a subsurface oxide phase as described in sec. 3.1.2. The dissociation process, together with the concurrent desorption of the precursor back into the gas phase, will define a steady state concentration of the precursor species, which, due to the small steady state concentration of the hydroxyl species, is still defined by Equation 2. Figure 6 indicates the concentration of adsorbed oxygen, $[O_{ad}]$, in excess of the chemisorbed oxygen coverage, at steady state; that is:

$$d[O_{ad}]/dt=2k'_a[P']n_s^2-k_1K[O_{ad}][H_{ad}]+k_{-1}[OH_{ad}]+k_2[OH_{ad}]^2=0 \qquad (19)$$

We will add the RHS of Equation 6, which is already assumed to have a negligible value (see above), to the above equation to obtain the following expression for dI^*/dt, which will also vanish under steady state conditions:

$$dI^*/dt=2k'_a[P']n_s^2-k_2[OH_{ad}]^2=0 \qquad (20)$$

Substituting for $[OH_{ad}]$ its equivalent expression from Equation 11, and remembering that at steady state $[H_{ad}]$ is constant, we find:

$$[O_{ad}]^2=2k_a\{k_{-1}/k_1Kk_2[H_{ad}]n_s\}^2[P']$$

or $$(I^*-I_f)^2 \alpha [P'] \qquad (21)$$

Equation 2 indicates that $[P']$ varies linearly with P_{O2}. Therefore, the magnitude of (I^*-I_f) at steady state should increase linearly with the square root of oxygen partial pressure, as is observed experimentally.

According to Equation 16, the rate of water formation, I_w, under the above steady state conditions is a function of $(I^*-I^*_f)^2$, and thus it is a linear function of P_{O2}. The results presented in Figure 5 are in reasonable agreement with this observation, considering the rather crude method of determining the relative changes in oxygen partial pressure which had to be employed (ion gauge reading); a slope of 0.8±0.1, instead of the expected value of unity, was obtained.

5- Discussion:

The results presented above demonstrate that once atomic hydrogen is present on a surface covered with more than one monolayer

of oxygen, the titration of the latter proceeds rapidly. Therefore, for hydrogen partial pressures of $1x10^{-5}$ torr or less, it is the slow (dissociative) adsorption of hydrogen molecules on the oxygen covered surface that prohibits the titration of oxygen at measurable rates. Benziger and Madix [23] have studied the influence of a number of surface contaminants on the adsorption of hydrogen on an Fe(100) surface. On a surface saturated with chemisorbed oxygen, they found that the necessary exposure to obtain a hydrogen coverage equivalent to that on a clean surface increased by more than three orders of magnitude. This difference is at least partly because of the reduced sticking probability of hydrogn on the oxygen covered surface [23], perhaps due to site blocking. Therefore, it may be expected that the titration reaction will have an appreciable rate at hydrogen partial pressures large enough to compensate for this apparent reduction of the sticking probability; a case that has been verified directly by the experiments of Vink et al. [5] (see sec. 1).

On the other hand, this decrease in the sticking coefficient of hydrogen may be only of secondary importance in explaining the stability of chemisorbed oxygen on this polycrystalline and the (100) [5a] surfaces of iron. This observation follows the finding that even the atomically adsorbed hydrogen (supplied by permeation) is incapable of removing the chemisorbed oxygen. Possible examples of other rate limiting factors for the titration of the chemisorbed oxygen include a high activation energy for the formation of OH from a chemisorbed oxygen atom, or a large barrier to the disproportionation of two such OH species, among others.

This is in contrast to the interaction of hydrogen with

chemisorbed oxygen on a number of other metallic surfaces, where complete titration takes place upon exposure of the surface to gas-phase hydrogen (e.g. on Pt [17,24], Ni [19,25], Pd [26,27], as well as Fe(110) [5b]).

The kinetic mechanism proposed here differs from that suggested by Vink et al. [5a] for the Fe(100) surface. Instead of the disproportionation process, their model assumes the direct reaction of the hydroxyl species with adsorbed hydrogen atoms to form water. On the other hand, both models require the intermediate OH species. The formation of hydroxyl radicals upon exposure of both polycrystalline [1,2] and (110) [3,4] surfaces of iron, as well as other metallic surfaces [28], to water has been confirmed directly by UPS [1,4], XPS [1,2], and EELS [3]. Also, in a recent study of the interaction of oxygen and hydrogen coadsorbed on a Rh(100) surface, temperature programmed electron energy loss spectroscopy made the direct observation of OH formed as the result of the above reaction possible [22].

The disproportionation model has been invoked previously for iron surfaces. Akimov [1] observed that annealing an iron surface, initially exposed to water at 75 K, in the 110-200 K range, resulted in the desorption of some of the adsorbed H_2O molecules concurrent with the transformation of others to OH species. At higher temperatures the OH species reacted and, in addition to producing water molecules, which desorbed, chemisorbed oxygen was formed. The author suggested the disproportionation mechanism for this process. On the Fe(110) surface, Baro and Erley [3] observed the dissociative adsorption of water at low coverages. Thermal processing of this

surface resulted in water desorption, and formation of residual to adsorbed oxygen as identified by EELS. Again, as suggested by the authors, the mechanism consistent with this observation is disproportionation, since the direct reaction of OH with a hydrogen adatom would not produce an adsorbed oxygen atom. Also, on an Fe(110) surface pre-saturated with chemisorbed oxygen, exposure to water at low temperature resulted in the adsorption of an amount of H_2O equal to that on the clean surface [4]. Thermal desorption spectroscopy indicated only the evolution of water, for which the authors postulated an OH disproportionation mechanism as confirmed here. At the end of the desorption experiment, only a concentration corresponding to a saturated layer of chemisorbed oxygen remained on the annealed surface. In contrast to the as-exposed surface, which showed the surface to be covered with OH, photoemission spectra of the annealed sample indicated only the presence of adsorbed oxygen.

In spite of the disagreement in the kinetic models, it is important to note that both this study and that of Vink et al. [5a], conclude that the one monolayer of oxygen adsorbed on top of the surface does not participate in the reaction with hydrogen. These are the only two such examples known to us, and in this regard the reader is reminded that x-ray diffraction from our polycrystalline sample indicated that the surface is, at least locally, vicinal to the (100) surface (i.e. a (429) orientation).

We have shown that, in the temperature range of this study, the formation (and desorption) of water due to reaction schemes I or II (section 4) is slow relative to disproportionation sequence. Due to the oxygen dissolution problem that was described earlier we did

not perform measurements at higher temperatures, which may favor these reaction paths.

The linear decrease of ln(B) versus I_o^*, indicates that it is the effective activation energy for the titration process which depends on the initial coverage. This is in partial agreement with the results of Benziger and Madix [23] who observed a decrease in the desorption energy of hydrogen in the presence of chemisorbed oxygen. Since the second-order rate constant for hydrogen desorption appears in the denominator of the expression for B (Equation 14b), a decrease in the desorption energy will be manifested as an increase in the activation energy for the overall reaction. However, this explanation is incapable of accounting for the dependence of B on the initial rather than the instantaneous, oxygen coverage. Alternatively, the reduction in apparent activation energy may be due to an effect of the initial coverage on the equilibrium constant, K, which describes the relationship between the coverage of the titratable oxygen atoms on the surface and the total concentration of these species. As described previously, the incorporation of adsorbed oxygen into the subsurface region is a non-activated process. Therefore, K can decrease if the activation energy for the reverse process - i.e. the return of an oxide anion to the surface - is increased due to a larger initial concentration of oxygen. Vink et al. [5a] have observed that for a constant initial coverage, the reduction process occurs more slowly if a sample that has been initially oxidized at room temperature is allowed to reconstruct during a high temperature anneal; the reconstruction increases the activation energy for titration. A similar process may be occuring here. Exposing the sample to more oxygen at a constant

partial pressure may provide more time for a reconstruction process. Alternatively the incorporation of more oxygen in the selvedge may result in a progressive disordering of the subsurface region, and thus make the reverse segregation process more difficult.

Finally, the agreement between the AES titration data and the QMS water desorption measurements, correlated through the proposed kinetic scheme, is a good indication that the Auger primary electron beam does not modify the titration process. In a similar study on Ni(110), Villarrubia and Ho [19] noted that the primary beam affects the kinetics of the reaction under conditions leading to slow titration rates, i.e. low temperature, low hydrogen partial pressure or an initially high oxygen coverage. For rapid reaction rates, on the other hand, they report that the reaction is insensitive to the primary electron beam, as observed here.

6- Summary:

The interaction of oxygen and hydrogen on a polycrystalline iron surface was studied in ultrahigh vacuum by a combination of mass spectrometry and Auger electron spectroscopy. In addition to exposing the surface to both reactant in the gas phase, a permeation cell was devised to introduce atomic hydrogen to the reaction surface by diffusion. The conclusions of these experiments are summarized below:

1- Due to its small sticking coefficient, hydrogen at partial pressures of less than 10^{-5} torr cannot reduce the oxidized surface of iron at measureable rates.

2- On the contrary, atomic hydrogen, introduced by permeation

from the back side of a thin iron slab, reacts to remove the adsorbed oxygen rapidly.

3- Regardless of temperature ($475 \leq T(K) \leq 625$) and the initial oxygen coverage (up to 3 monolayers), a final monolayer of chemisorbed oxygen remains untitrated by hydrogen; no reaction is observed when the initial coverage of oxygen is less than one chemisorbed monolayer. This phenomenon, which has also been reported for the removal of oxygen from Fe(100) by hydrogen in the gas phase, is not due to the kinetics of hydrogen adsorption and may be due to the thermodynamic stability of the chemisorbed oxygen on these particular surfaces of iron.

4- The titration of oxygen in excess of one monolayer involves the initial formation of an intermediate hydroxyl group from the coadsorbed oxygen and hydrogen atoms, followed by the disproportionation of two OH species to form water, which desorbs upon formation.

5- An average energy of 16 Kcal/mole was calculated for the overall titration process. Of this total energy, 8.5 Kcal/mol is due to hydrogen permeation.

Acknowledgement:

This work was supported in part by ARO under Contract No. DAAL003-86-K-0076, and in part by the chemistry program of ONR. This support is gratefully acknowledged. The work is based on a thesis presented by one of us (M.A.) in partial fulfillment of the requirements for the Ph.D. degree at Rensselaer Polytechnic Institute.

Figure Captions:

Figure 1 The kinetics of oxygen titration for various initial oxygen coverages at 550 K. Hydrogen permeation started at time=0.

Figure 2 The kinetics of oxygen titration at: x 475 K, + 525 K, and 625 °K, for a constant initial coverage. The solid curves correspond to the fit of the data to the model discussed in sec. 4 (eqn. 14).

Figure 3 Isothermal dissolution of oxygen into the bulk at 575 and 625 K, in vacuum. The initial oxygen coverage in these experiments was the same as in those shown in fig. 2.

Figure 4 The evolution of water during a titration experiment at 625 K as measured by the mass spectrometer. Hydrogen permeation was initiated at t=30 sec.

Figure 5 The rate of water formation at 550 K for steady state hydrogen permeation, versus oxygen partial pressure.

Figure 6 Oxygen concentration (I^*) in excess of I^*_f, during the steady state permeation of hydrogen, versus oxygen partial pressure (uncalibrated mass spectrometer output).

Figure 7 Arrhenius plot of the reaction rate constant B (AES data, eqn. 14) versus temperature.

Figure 8 The rate of H_2O formation, I_w, measured by mass spectrometry during titration experiments at: 500 and 625 °K, versus the rate calculated from the AES data. Solid lines indicate the least square fits to the data.

Figure 9 Arrehenius plot of the reaction rate constant B', obtained from the QMS data and eqn. 16 in the text, versus temperature.

Figure 10 The titration rate constant, B, versus the initial oxygen coverage, I^*_o, for H_2 ( ) and D_2 ( ) at 550 K.

References

1-A. G. Akimov, Electrokhimiya (Soviet Electrochem.), 15 (1979) 1301;

2-M. W. Roberts and P. R. Wood, J. Electron Spectroscopy and Related Phenomena, 11 (1977) 431;

3-A. M. Baro and W. Erley, J. Vac. Sci. Technol., 20 (1982) 580;

4-D. J. Dwyer, S. R. Kelemen, and A. Kaldor, J. Chem. Phys., 76 (1982) 1832;

5a-T. J. Vink, J. M. Der Kinderen, O. L. J. Gijzeman, and J. W. Geus, Applied Surface Sci., 26 (1986) 367;

5b-T. J. Vink, S. J. M. Sas, O. L. J. Gijzeman, and J. W. Geus, J. Vac. Sci. Technology A 5 (1987) 1028;

6-C. M. A. M. Mesters, T. J. Vink, O. L. J. Gijzeman, and J. W. Geus, Surface Sci., 135 (1983) 428;

7-J. Volkl and G. Alefeld, in Hydrogen in Metals I, ed. J. Volkl and G. Alefeld (1978, Springer-Verlag);

8-M. Arbab and J. B. Hudson, Applied Surface Sci., 29 (1987) 1;

9-M. Arbab and J. B. Hudson, submitted to Surface Science;

10-M. Seo, J. B. Lumsden, and R. W. Staehle, Surface Sci., 50 (1975) 541;

11-P. B. Needham and T. J. Driscoll, J. Vac. Sci. Technology, 11 (1974) 278;

12-T. J. Vink, J. M. Der Kinderen, O. L. J. Gijzeman, J. W. Geus, and J. M. Van Zoest, Applied Surface Sci., 26 (1986) 357;

13- K. O. Legg, F. Jona, D. W. Jepsen, and P. M. Marcus, Phys. Rev. B, 16 (1977) 5271;

14-F. P. Fehlner and N. F. Mott, Oxid. Met., 2 (1970) 59.

15-R. Gorte and L. D. Schmidt, Surface Sci., 102 (1981) 388;

16-L. E. Davis, N. C. MacDonald, P. W. Palmberg, G. E. Riach, and L. E. Weber, Handbook of Auger Electron Spectroscopy, 2nd ed., (1976, Physical Electronics);

17-P. R. Norton, in: The Chemical Physics of Solid Surfaces and Heterogeneous Catalysis, Vol. 4, eds. D. A. King and D. P. Woodruff (1982, Elsevier);

18a-A. Anderson, Surface Sci., 105 (1981) 159; b-N. C. Debnath and A. Anderson, Surface Sci., 128 (1983) 61;

19-J. S. Villarubia and W. Ho, Surface Sci., 144 (1984) 370;

20-N. R. Quick and H. H. Johnson, Acta Metall., 26 (1978) 903;

21-E. A. Kurz and J. B. Hudson, Surface Sci., 195 (1988) 15;

22-B. A. Gurney and W. Ho J. Chem. Phys., in press;

23-J. Benziger and R. J. Madix, Surface Sci., 94 (1980) 119;

24-J. L. Gland, G. B. Fisher, and E. B. Kollin, J. Catalysis, 77 (1982) 263;

25- A. Benninghoven, P. Beckmann, K. H. Muller, and M. Schemmer, Surface Sci., 89 (1979) 701;

26-L. G. Petersson, H. M. Dannetun, and I. Lundstrom, Surface Sci., 161 (1985) 77;

27-T. Engel and H. Kuipers, Surface Sci., 90 (1979) 181;

28-G. B. Fisher and B. A. Sexton, Phys. Rev. Lett., 44 (1980) 683;

29-J. Crank, The Mathematics of Diffusion, 2nd ed. (1975, Clarendon Press);

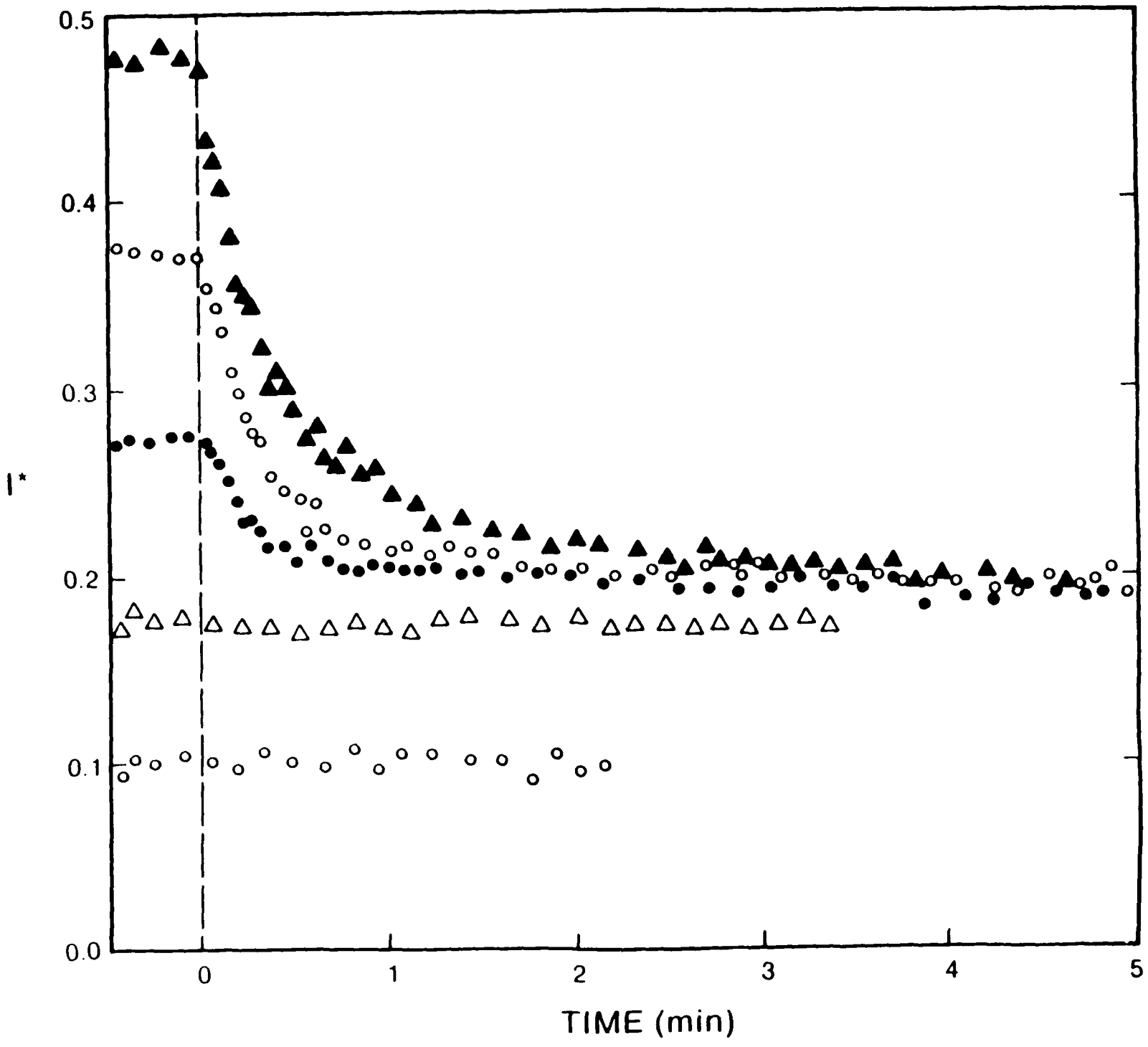
0.5
0.4
0.3
0.2
0.1
0.0
I*
0
1
2
3
4
5
TIME (min)

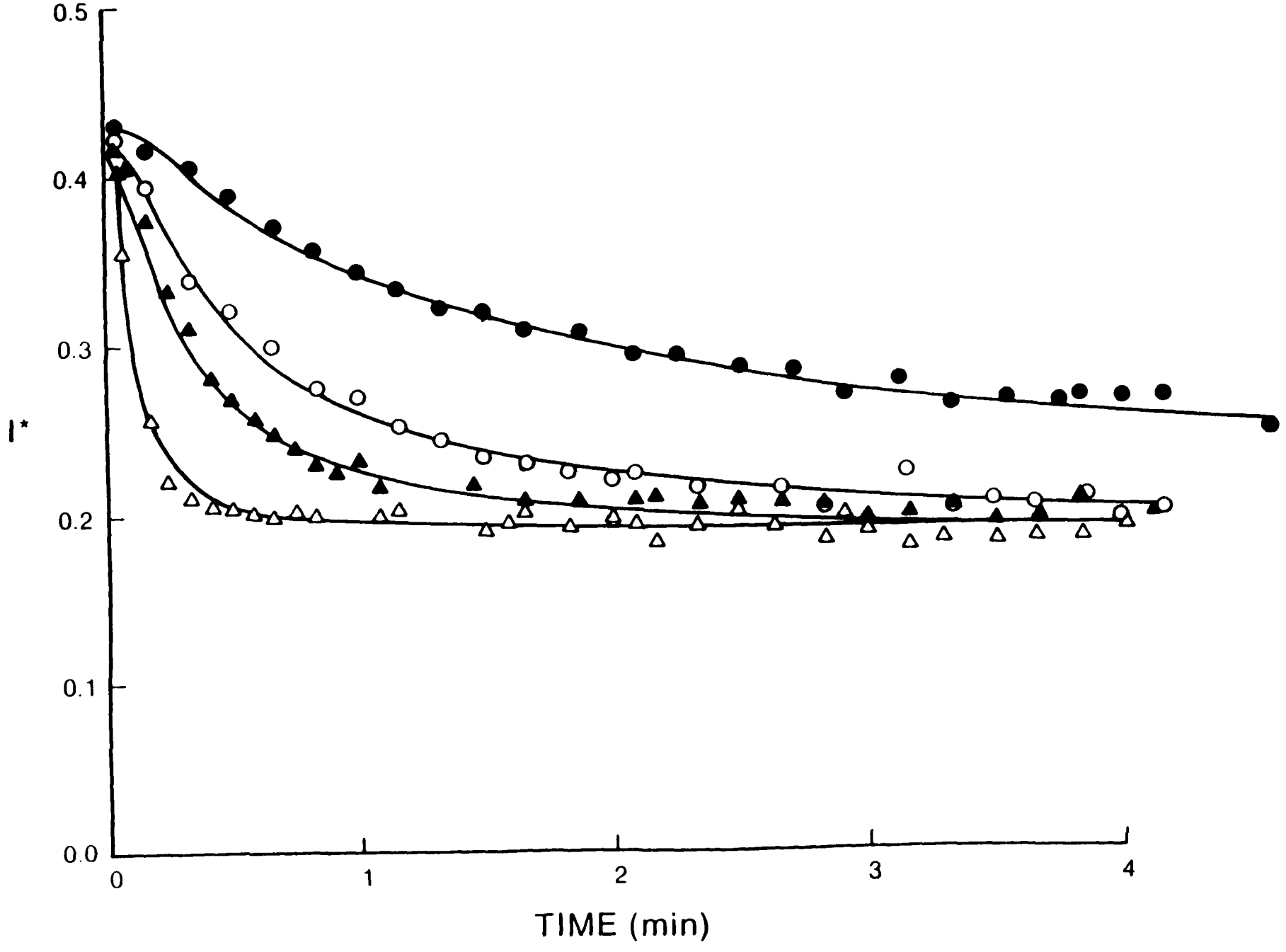
0.5
0.4
0.3
0.2
0.1
0.0
I*
0
1
2
3
4
TIME (min)

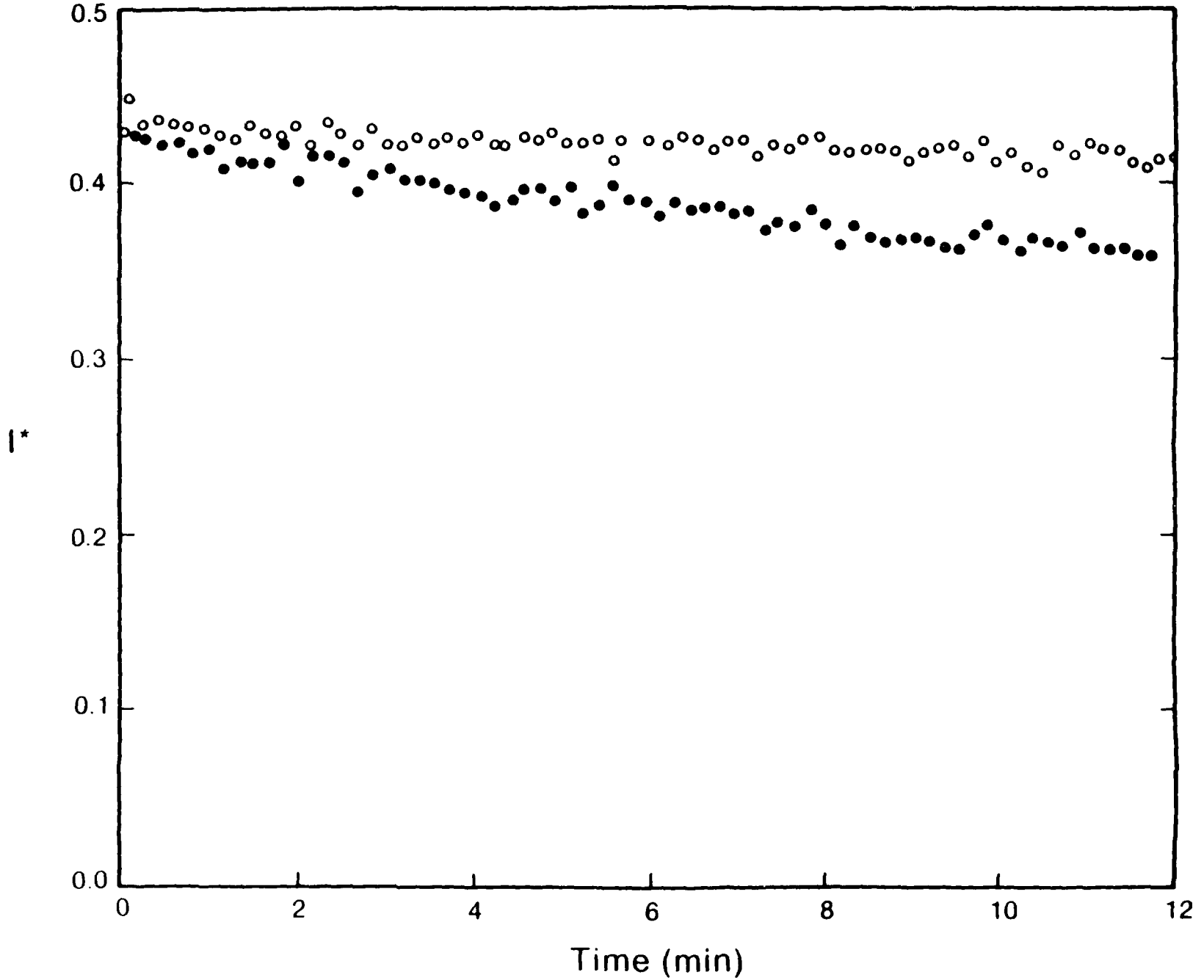
0.5
0.4
0.3
0.2
0.1
0.0
I*
0
2
4
6
8
10
12
Time (min)

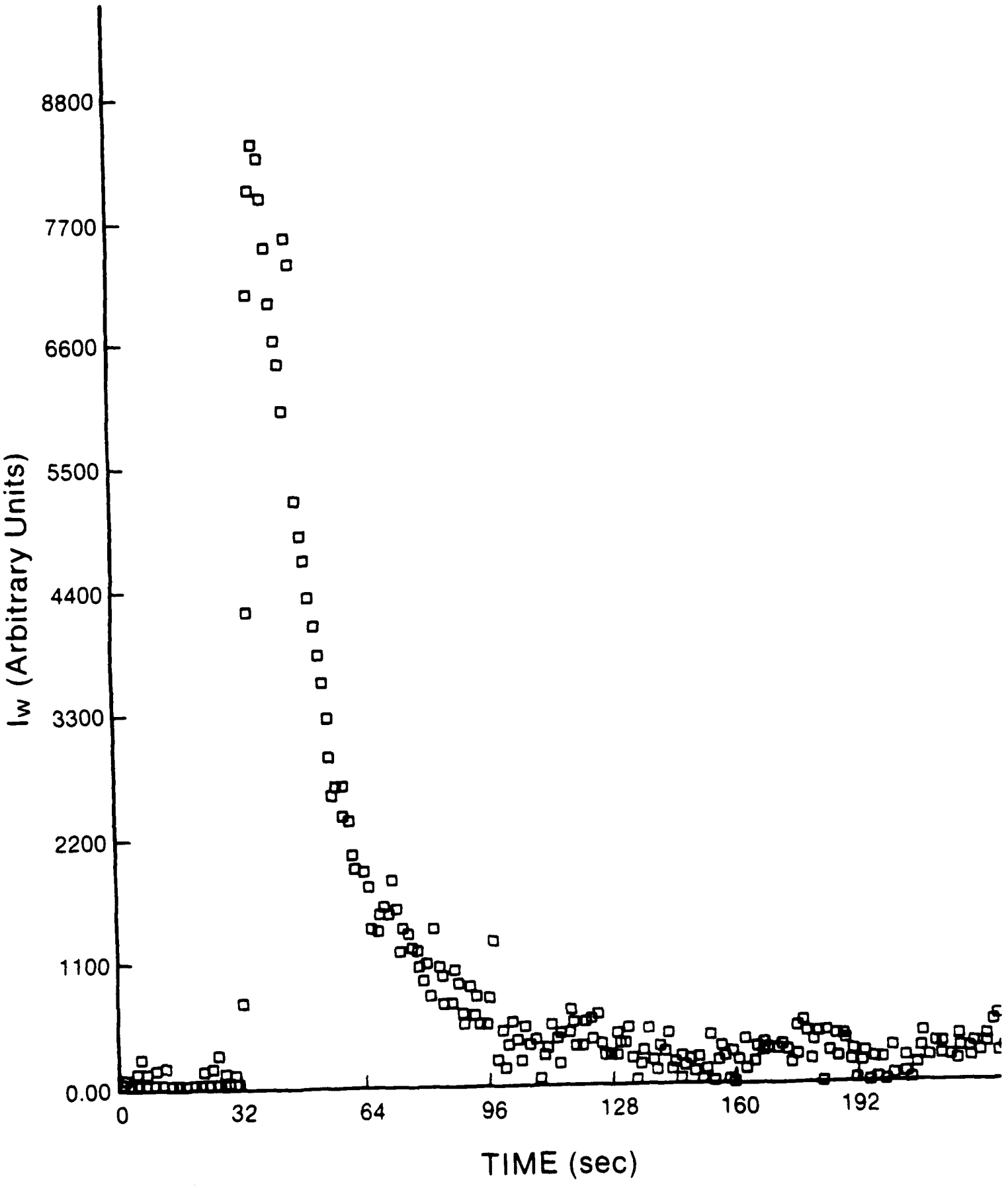
8800
7700
6600
5500
4400
3300
2200
1100
0.00
I_W (Arbitrary Units)
0
32
64
96
128
160
192
TIME (sec)

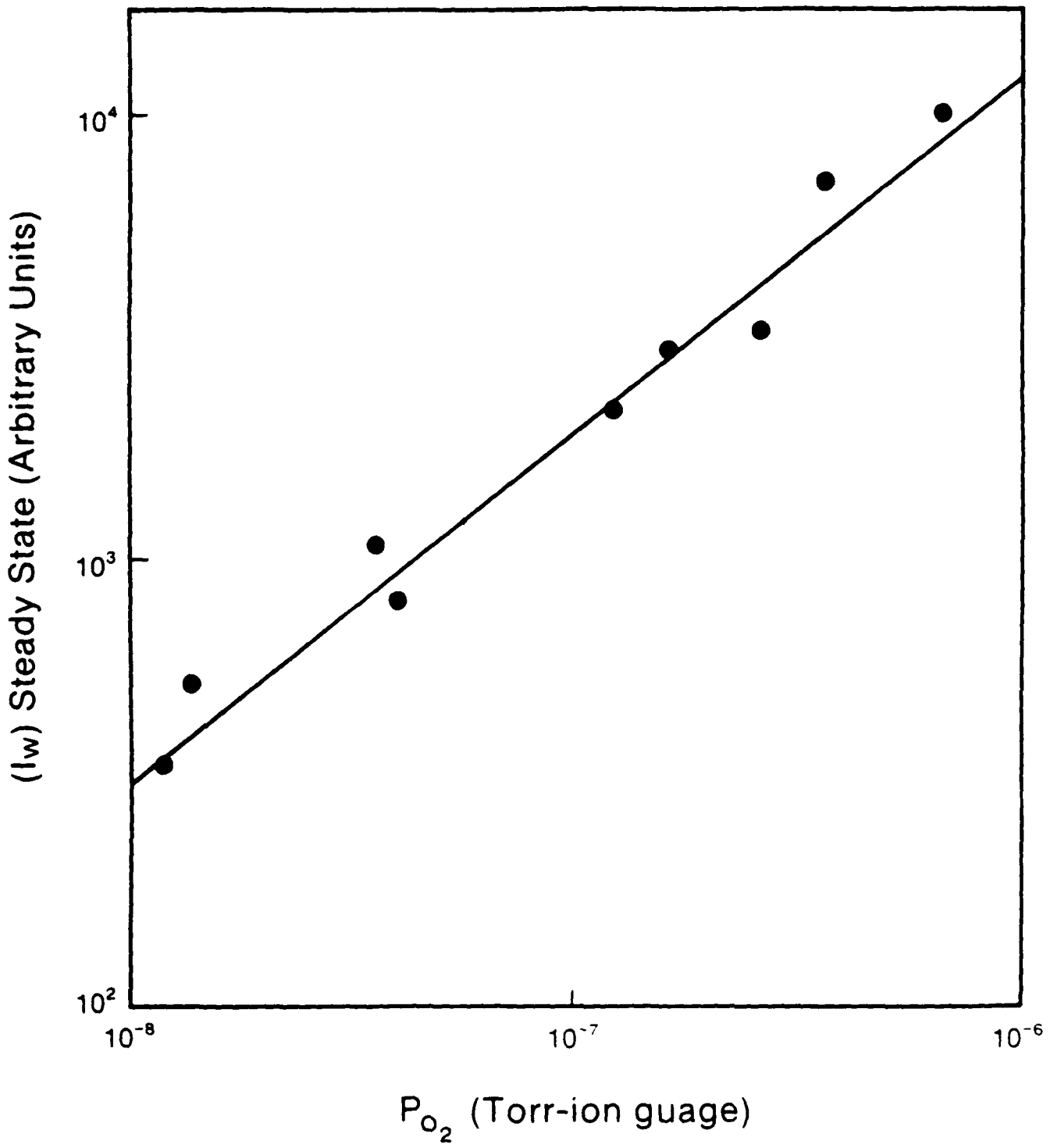
10^4
10^3
10^2
(I_w) Steady State (Arbitrary Units)
10^{-8}
10^{-7}
10^{-6}
P_{O_2} (Torr-ion guage)

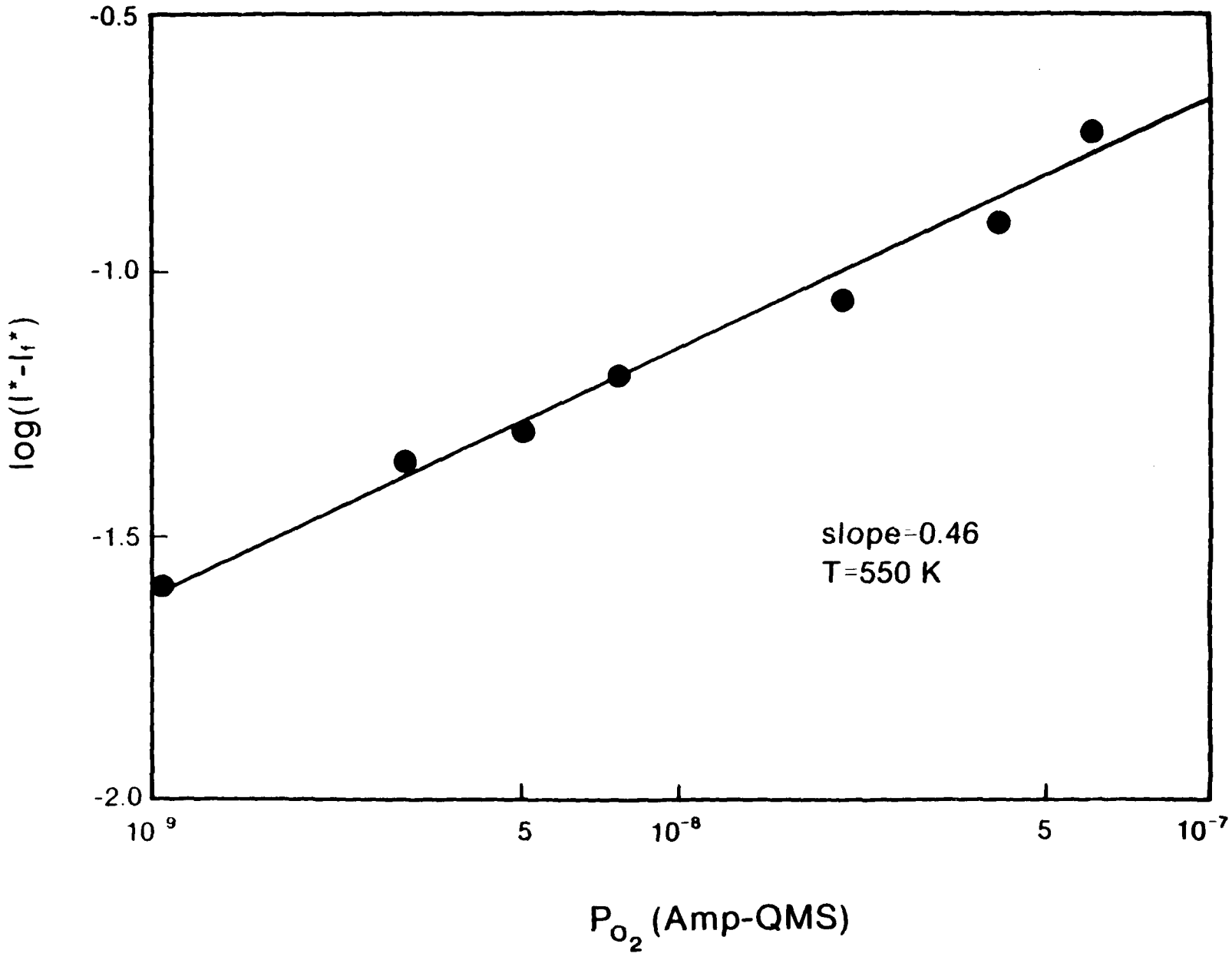
-0.5
-1.0
-1.5
-2.0
log(I*-I_f*)
10^-9
5
10^-8
5
10^-7
slope=0.46
T=550 K
P_O2 (Amp-QMS)

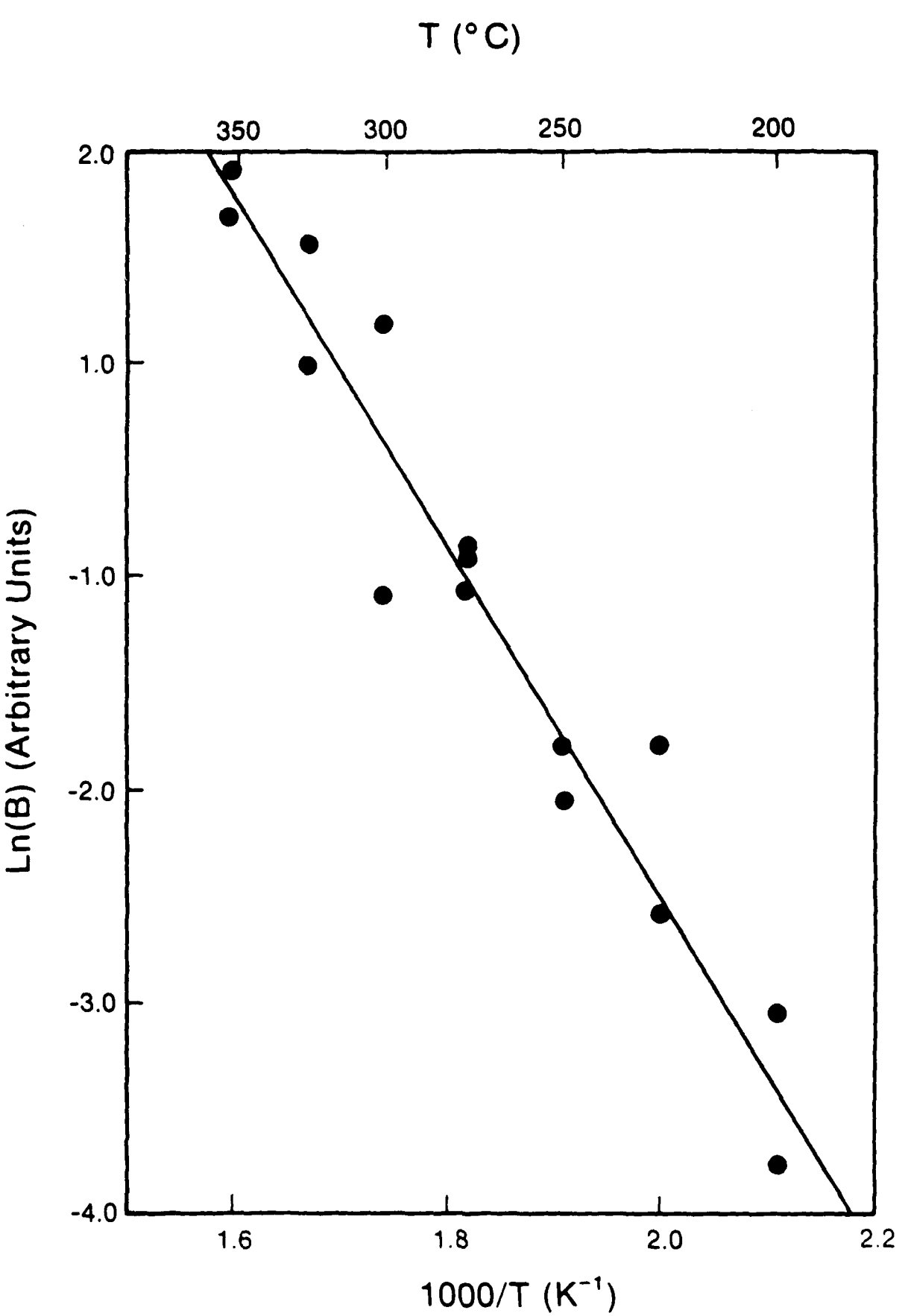
T (°C)
350
300
250
200
2.0
1.0
-1.0
-2.0
-3.0
-4.0
Ln(B) (Arbitrary Units)
1.6
1.8
2.0
2.2
1000/T (K⁻¹)

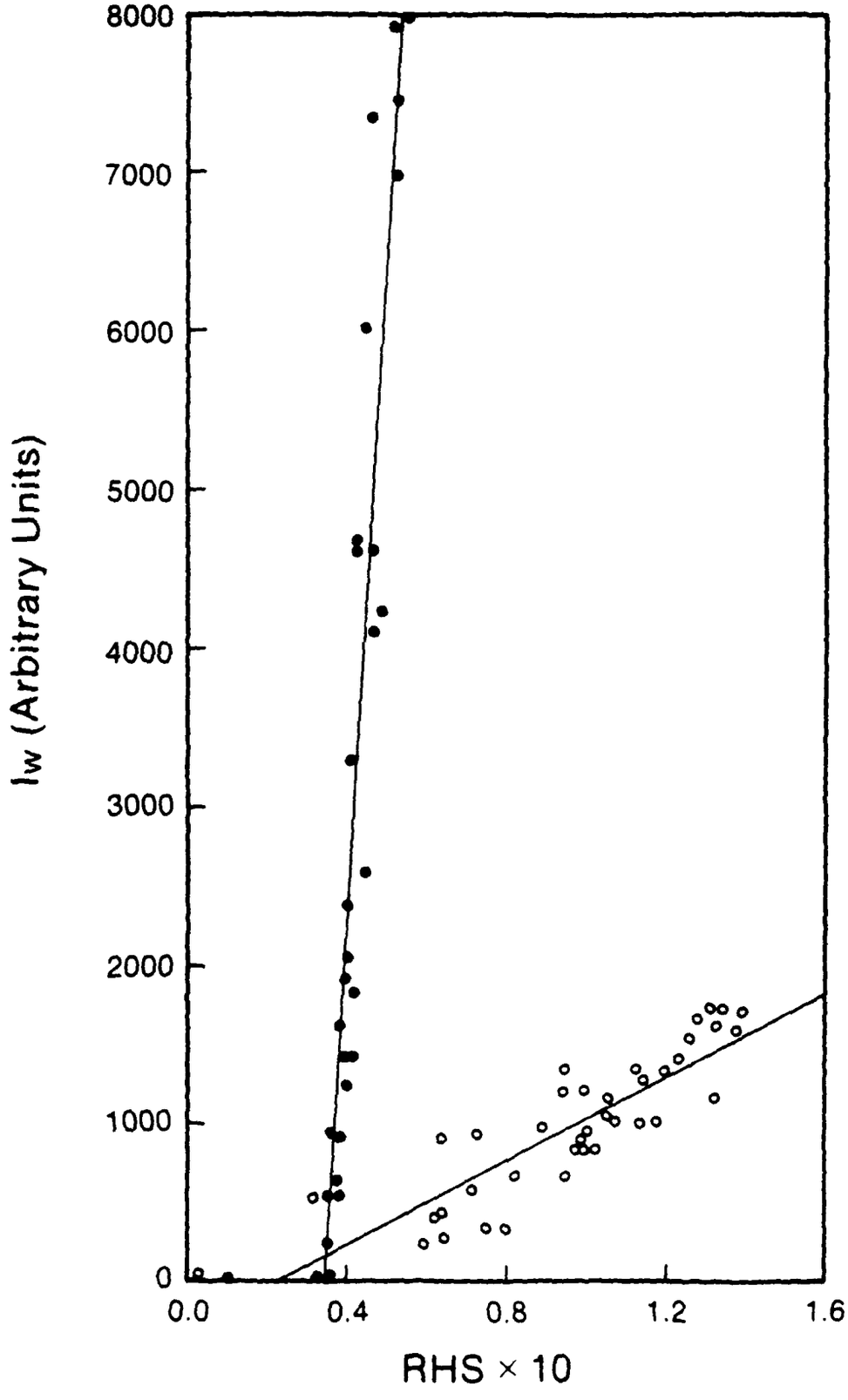
8000
7000
6000
5000
4000
3000
2000
1000
0
I_W (Arbitrary Units)
0.0
0.4
0.8
1.2
1.6
RHS × 10

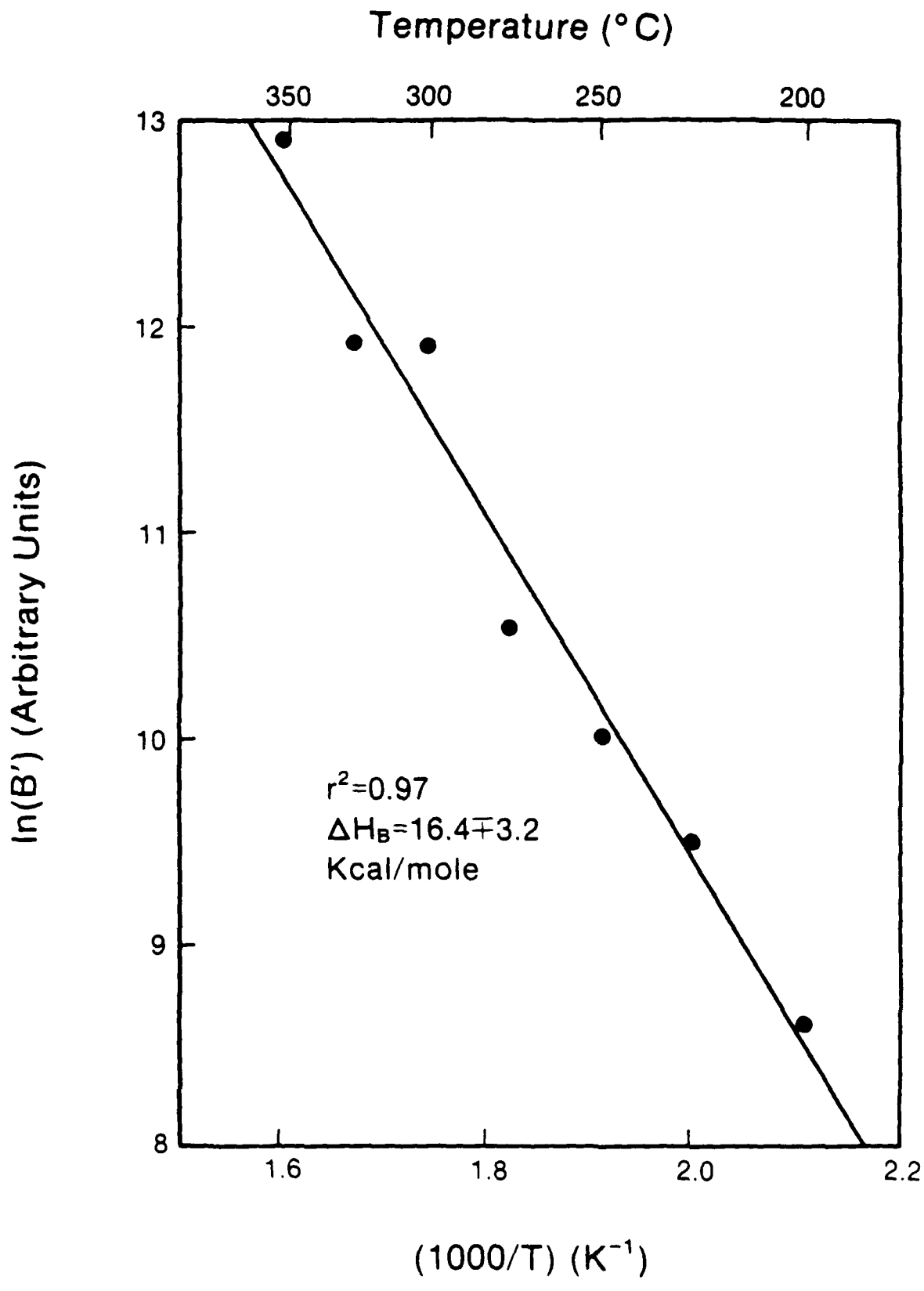
Temperature (°C)
350
300
250
200
13
12
11
10
9
8
ln(B') (Arbitrary Units)
r^2=0.97
ΔH_B=16.4∓3.2
Kcal/mole
1.6
1.8
2.0
2.2
(1000/T) (K^{-1})

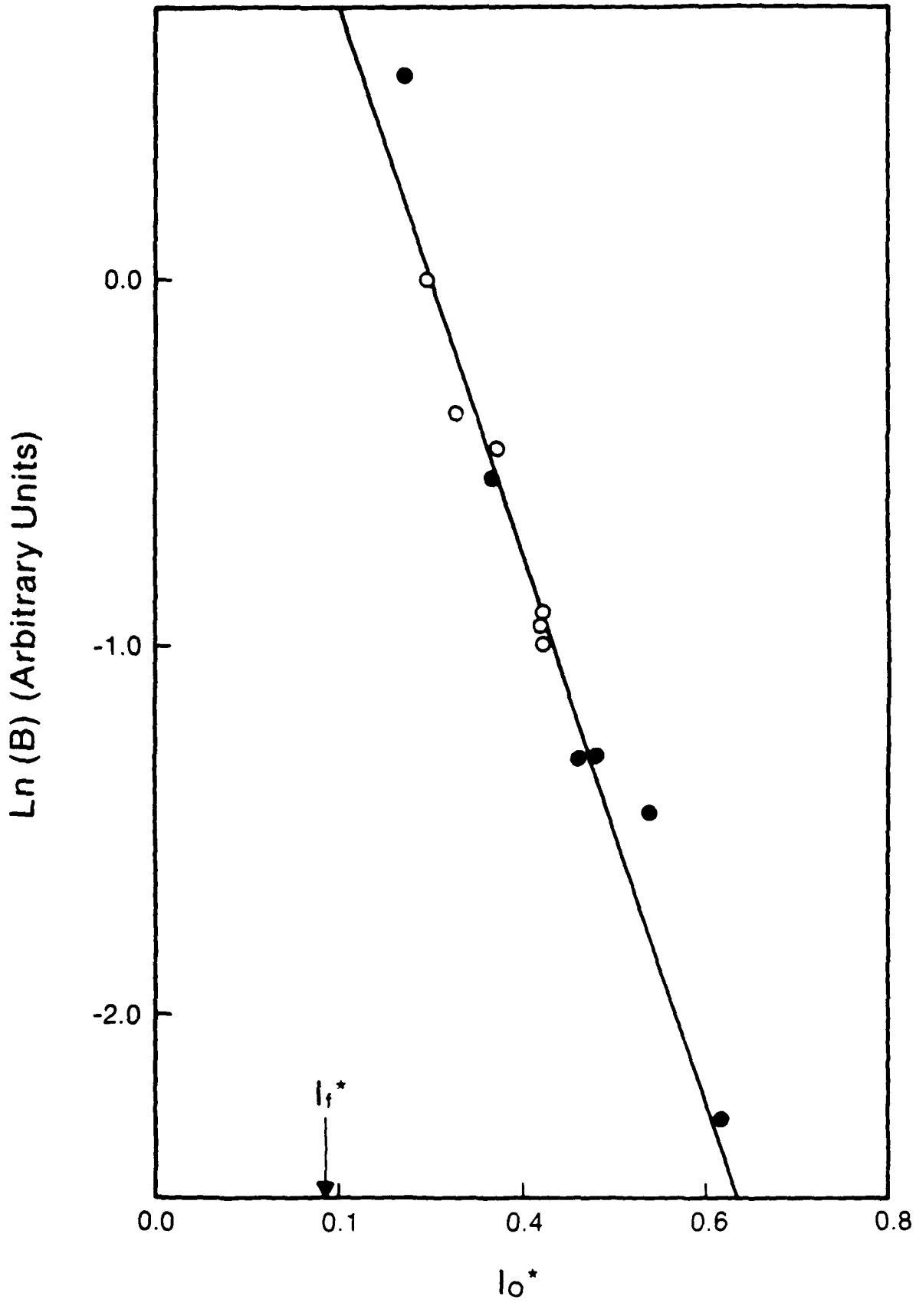
Ln (B) (Arbitrary Units)
0.0
-1.0
-2.0
I_f^*
0.0
0.1
0.4
0.6
0.8
I_o^*